

Update on MAC End-Station at ELI Beamlines Facility

E. KLIMEŠOVÁ^{a,*}, A.H. ROOS^a, Z. HOQUE^a, N. SMIJESH^a,
R.J. SQUIBB^b, H. COUDERT-ALTEIRAC^b, R. FEIFEL^b,
J. ANDREASSON^a AND M. KRİKUNOVA^{a,c}

^a*ELI Beamlines facility, The Extreme Light Infrastructure ERIC, Za Radnicí 835, 252 41 Dolní Břežany, Czech Republic*

^b*Attohallen Facility, University of Gothenburg, Department of Physics, Origovgen 6B, SE-412 58 Gothenburg, Sweden*

^c*Technical University of Applied Sciences, Hochschulring 1, 15745 Wildau, Germany*

Doi: [10.12693/APhysPolA.145.118](https://doi.org/10.12693/APhysPolA.145.118)

*e-mail: eva.klimesova@eli-beams.eu

The MAC end-station at the ELI Beamlines facility is a multipurpose user's station for atomic, molecular, and optical sciences and coherent diffractive imaging. The technical design of the station, the available instruments, and an overview of the whole beamline have been published in *Eur. Phys. J. Spec. Top.* **230**, 4183 (2021). Here, we address ongoing upgrades of the MAC end-station that will provide users with advanced capabilities for beam manipulation and electron/ion detection. The upgrades include (i) the installation of a beam preparation chamber in front of the MAC chamber, (ii) a magnetic bottle electron spectrometer with high collection and detection efficiency and high energy resolution, and (iii) an event-driven TPX3CAM detector for velocity map imaging spectrometer, which provides both spatial and temporal information for each pixel. We present results from the first commissioning measurements with these instruments, confirming their performance for state-of-the-art experiments in atomic, molecular, and optical sciences.

topics: atomic and molecular sciences, lasers, electron and ion spectroscopy

1. Introduction

High harmonic generation (HHG) is a well-established technique to produce coherent extreme ultraviolet (XUV) radiation with excellent properties, such as high temporal and spatial coherence, femtosecond pulse duration, high intensity, synchronization with other laser beams, and the possibility to select a single harmonic by a monochromator [1–4]. The applications of femtosecond high harmonics include time-resolved studies of chemical processes [5–7], tracking and controlling ultrafast electron dynamics in atoms [8, 9], probing chiral molecules in the gas phase [10], or investigations of transient phenomena in nanoscale quantum systems [11–15].

The HHG beamline at ELI Beamlines facility near Prague, Czech Republic [4, 14], is primarily driven by an in-house L1 laser (central wavelength 830 nm, pulse duration 15 fs, energy per pulse up to 100 mJ, repetition rate 1 kHz [16]) and provides XUV pulses in the photon energy range of 20–100 eV for user experiments in different research areas. We address the user end-station MAC at the HHG beamline — a multipurpose station for atomic, molecular, and optical sciences (AMO) and coherent diffractive imaging (CDI) [17]. At MAC,

the HHG beam synchronized with an auxiliary laser beam is used to unveil ultrafast electron and ion dynamics in low-density targets, such as atoms [9, 18], molecules, helium nanodroplets [14, 15], or nanoparticles [19]. Moreover, CDI studies on solid targets are possible at MAC [20]. The technical design of the MAC station, available beams, sample delivery systems, and diagnostics have been described in detail in [17].

To advance experiments at the MAC end-station and provide the user community with additional capabilities, several upgrades are currently underway. First, a new beam preparation chamber (so-called B4MAC) will be installed to offer more complex options for the manipulation and focusing of the beams. A magnetic bottle electron spectrometer (MBES), currently being commissioned, will provide high collection and detection efficiency of ions and electrons, high energy resolution, and an option for coincidence electron–ion detection. Finally, the current velocity map imaging (VMI) spectrometer has been upgraded with a TPX3CAM detector to enable fast and efficient spatial and temporal signal acquisition. In this contribution, we describe these upgrades, show the results of the first measurements, and discuss the user-access policies at the ELI Beamlines facility.

2. MAC end-station upgrades

An overview of the MAC end-station with different diagnostics instruments is shown in Fig. 1. The large rectangular chamber on the left is the B4MAC chamber for focusing and manipulation of multiple beams. The diagnostic instruments on MAC are MBES, VMI, and XUV spectrometers. Apparatuses for sample delivery (molecular beam or cluster source) are not shown; they are normally installed in a horizontal orientation. The setup is modular and can be adjusted for a specific user experiment.

2.1. Beam preparation chamber B4MAC

For time-resolved experiments at the MAC end-station, an XUV beam is overlapped with a synchronized auxiliary beam in MAC. The auxiliary beam can be the fundamental with a wavelength of around 800 nm or its second or third harmonic. In the current setup, XUV beam forward-focusing with an ellipsoidal mirror [9] and XUV beam back-focusing with a spherical mirror [14] have both been implemented. Pump-probe experiments have been performed with the forward-focusing setup. CDI has been performed inside the MAC chamber.

To offer more options and more space for beam manipulation and focusing, a B4MAC beam preparation chamber with a decoupled optical breadboard will be installed (Fig. 2). Focusing geometries possible with B4MAC include:

1. XUV forward-focusing with ellipsoidal mirror, typically after the beam passes the monochromator. XUV focal spot size is around $35 \times 50 \mu\text{m}$ full width at half maximum. Auxiliary beam(s) can be coupled collinearly or at a small angle with the XUV beam.
2. XUV back-focusing with off-axis parabola; focal spot size of a few micrometers. This geometry is foreseen to be utilized mainly for CDI on solid targets in the B4MAC chamber, providing enough space for CDI setup with diagnostics.
3. Two XUV beam experiments (anticipated in the future).
4. XUV back-focusing with a spherical mirror in MAC (not shown in Fig. 2). Focal spot size can be as small as $\sim 1 \mu\text{m}$. In this case, the multilayer spherical mirror is placed inside the MAC chamber. Different coatings can be used depending on the users' needs.

Moreover, thanks to many useful ports on the B4MAC chamber and a large optical breadboard decoupled from the vacuum system, custom user-specific geometries can be implemented there.

2.2. Magnetic bottle electron spectrometer

To offer high electron energy resolution and high collection efficiency, an MBES for the MAC end-station is now being commissioned. It has been developed and commissioned in collaboration with the group of Raimund Feifel, University of Gothenburg, Sweden, and is based on the design presented in [21]. The main components of the MBES are a strong permanent magnet placed close to the interaction region, followed by a flight tube and a microchannel plate (MCP) detector (Fig. 3). The permanent magnet creates a strong magnetic field that collects basically all electrons emitted in the 4π solid angle.

The electron flight tube is surrounded by a solenoid to guide electrons on their way to the MCP detector. The length of the flight tube of 2 m ensures a high spectral resolution. An optional electrostatic lens assembly can be attached to the flight tube for high-resolution ion detection. The MCP detector (Hamamatsu, model F9892-31) has an open area ratio of more than 90%, leading to a large detection efficiency.

An example photoelectron spectrum from the commissioning experiments in Gothenburg is shown in Fig. 4. In this measurement, atomic Xe was ionized by a laser with a photon energy of 4.8 eV (4th harmonic of 1030 nm laser), 160 fs pulse duration, and a repetition rate of 3 kHz. The two photoelectron lines originate in 3-photon ionization of the Xe atom from its $5p_{1/2}$ and $5p_{3/2}$ states, respectively. The measured spacing between the lines corresponds to the spin-orbit splitting of the Xe $5p$ shell. From the full width at half maximum of the $5p_{3/2}$ line, one can infer a spectral resolution of about $E/\Delta E = 60$ in this photoelectron energy range.

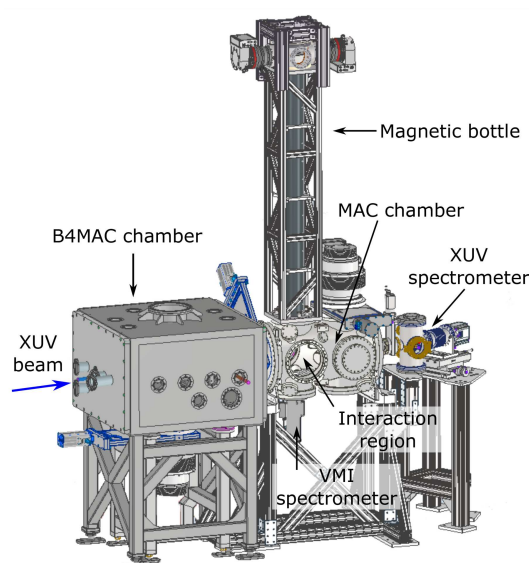


Fig. 1. Schematic view of the MAC end-station with different diagnostics instruments. Sample delivery systems are not shown.

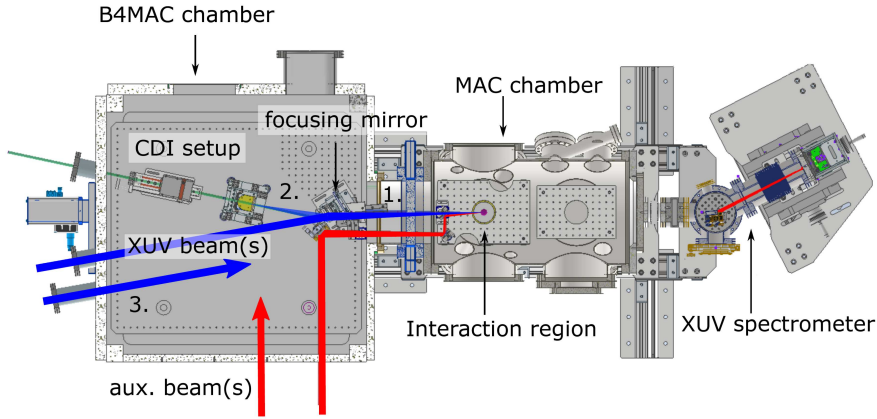


Fig. 2. Schematics of the B4MAC and MAC chambers with the XUV and auxiliary beams. For a description of different geometries (1–3), see the text.

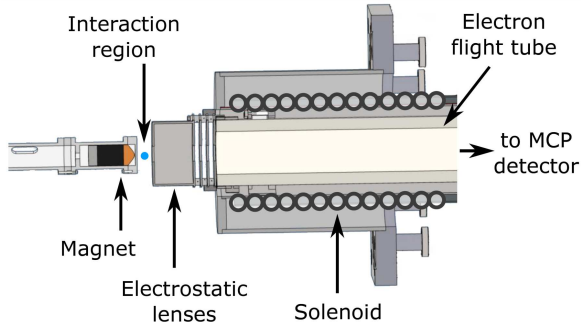


Fig. 3. A schematic drawing of the magnetic bottle electron spectrometer in the electron-only configuration. Electrons are confined by the combined magnetic field of the permanent magnet and the solenoid and fly through the flight tube to the MCP detector.

MBES can be operated in two primary configurations, namely electron detection only, or electron-ion coincidence. In the latter setup, electrodes for ions and an ion detector are added to the instrument [22]. Pulsed voltages are used to extract ions after the electrons leave the interaction region (i.e., around 100 ns after ionization). Xe ions detected in coincidence with electrons are shown in the inset of Fig. 4. Six Xe isotopes are resolved. The seventh Xe isotope with a mass of 130 amu with an abundance of 4% is in the tail of 129 amu isotope. The MBES will be installed on the MAC chamber in a vertical orientation and will provide an efficient tool for electron spectroscopy and simultaneous electron and ion detection.

2.3. VMI spectrometer with TPX3CAM

The VMI spectrometer at the MAC end-station (Eppink and Parker design [23], manufactured by Photek) has been originally equipped with a CMOS camera (IDS, 166 frames per second). While

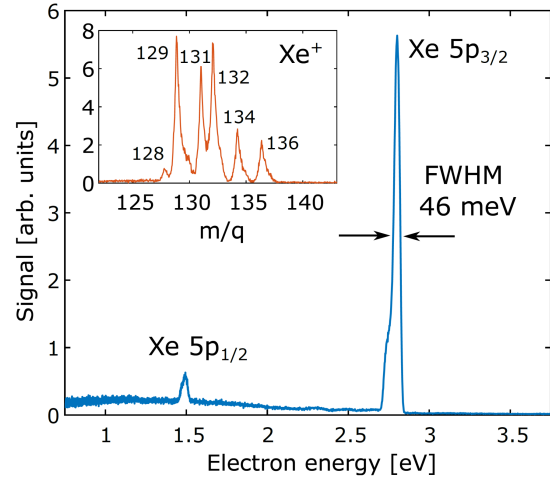


Fig. 4. Photoelectron spectrum measured with magnetic bottle electron spectrometer. Xe atoms were ionized with an intense laser (photon energy 4.8 eV, repetition rate 3 kHz, pulse duration 160 fs). Photoelectrons created by 3-photon ionization of Xe $5p_{1/2}$ and $5p_{3/2}$ states are indicated. Inset shows Xe^+ ion mass spectrum detected in coincidence with electrons. Individual Xe isotopes are indicated.

providing high collection efficiency and good energy and angular resolution, the data acquisition speed is limited by the camera readout, and gating is needed to detect specific ion species. An upgrade of the VMI consists of replacing the CMOS camera with an event-driven TPX3CAM detector (Amsterdam Scientific Instruments) [24, 25]. TPX3CAM is based on Timepix3 chip technology, where each hybrid pixel of the detector records both the intensity (related to time-over-threshold (ToT)) and time-of-arrival (ToA) of each event.

Employing TPX3CAM, one can simultaneously detect the time-of-flight spectrum (mass spectrum) and a velocity map image of each ion species. Thus, images of all ion species can be

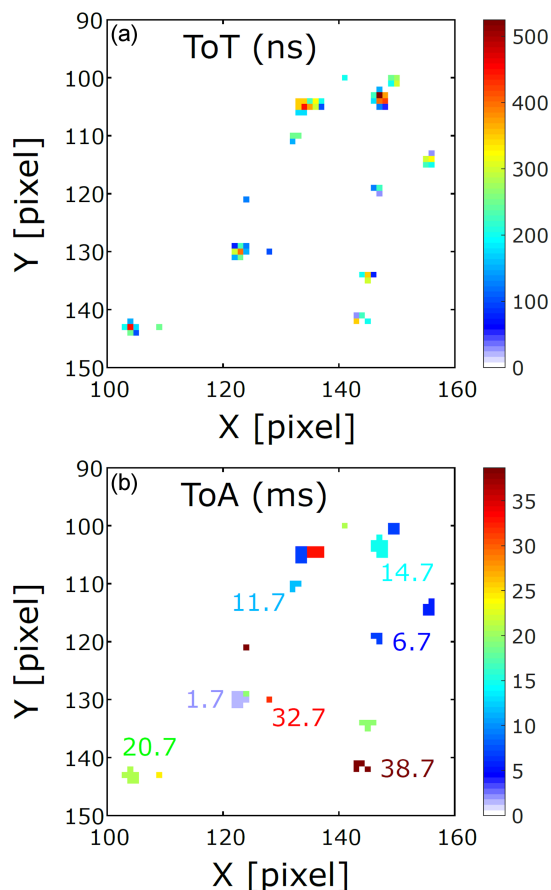


Fig. 5. Example of TPX3CAM pixel data. Electrons emitted from background gas in the MAC chamber ionized with an intense NIR beam at a 1 kHz repetition rate were detected. (a) Zoom on a ~ 40 ms measurement displaying the ToT of each pixel. (b) Same image as in (a) but showing ToA. Times of arrivals of several hits are indicated next to them.

recorded simultaneously, allowing for coincidence or covariance analysis to give complete information on the fragmentation pathways of the system under study [26, 27]. The ToA time bin of 1.56 ns is sufficiently small to resolve ion time-of-flight well, but becomes limiting for 3D electron detection.

An example measurement with TPX3CAM is shown in Fig. 5. Background gas in the MAC chamber was ionized by an intense near-infrared (NIR) laser beam at a 1 kHz repetition rate, and electrons were detected by the VMI spectrometer with TPX3CAM. TPX3CAM readout is event-based, so only hits arriving at the detector are registered, resulting in efficient data storage. For each event, both the ToT (proportional to the intensity, Fig. 5a) and ToA (Fig. 5b) are registered. One can see that the arrivals of different hits are spaced by 1 ms, corresponding to electrons created by different laser shots at the 1 kHz repetition rate. This measurement confirms the operation of TPX3CAM with

the VMI spectrometer, detecting both spatial and temporal information and offering fast and efficient data acquisition.

3. User access

The MAC end-station is a part of the ELI Beamlines facility [28], operated within the Extreme Light Infrastructure ERIC [29]. The ELI Beamlines facility is a user center providing access to high-power, high-repetition-rate laser systems and secondary sources. Access to the ELI Beamlines facility is free, competitive, and open to the international user community. Proposals are evaluated by international peer-review panels composed of independent peer reviewers. To find more information and apply for beamtime, visit the ELI ERIC user portal [29].

4. Conclusions

The MAC end-station is a multipurpose, modular instrument for a wide user community in the field of AMO sciences and CDI. It is operational and open for user access. Several experiments at MAC have already revealed intricate fast processes in atoms [9, 18], molecules, helium nanodroplets [14, 15], and nanoparticles [19]. We have presented ongoing upgrades of the MAC end-station, i.e., a B4MAC chamber for complex beam manipulation, an MBES for efficient and well-resolved electron detection, and a TPX3CAM on VMI spectrometer for simultaneous time and position data acquisition. The presented results demonstrate the functionality of these instruments, offering state-of-the-art technology for complex investigations.

Acknowledgments

The authors thank the staff of the ELI Beamlines Facility, a European user facility operated by the Extreme Light Infrastructure ERIC, for their support and assistance. This work was supported by the project “Advanced research using high-intensity laser produced photons and particles” (ADONIS) (CZ.02.1.01/0.0/0.0/16 019/0000789) and “Structural dynamics of biomolecular systems” (ELIBIO) (CZ.02.1.01/0.0/0.0/15 003/0000447), both from the European Regional Development Fund and the Ministry of Education, Youth and Sports. This publication is also based upon the work of COST Action CA21101 “Confined molecular systems: From a new generation of materials to the stars” (COSY) supported by COST (European Cooperation in Science and Technology). The work relating to MBES development and commissioning has been financially supported by the Swedish Research Council (VR), the Olle Engkvist Foundation, and the Knut and Alice Wallenberg Foundation, Sweden.

References

- [1] F. Calegari, G. Sansone, S. Stagira, C. Vozzi, M. Nisoli, *J. Phys. B At. Mol. Opt. Phys.* **49**, 062001 (2016).
- [2] L. Young, K. Ueda, M. Gühr et al., *J. Phys. B At. Mol. Opt. Phys.* **51**, 032003 (2018).
- [3] M. Reduzzi, P. Carpeggiani, S. Kühn et al., *J. Electron Spectrosc. Relat. Phenom.* **204**, 257 (2015).
- [4] O. Hort, M. Albrecht, V.E. Nefedova et al., *Opt. Express* **27**, 8871 (2019).
- [5] A.D. Smith, E.M. Warne, D. Bellshaw et al., *Phys. Rev. Lett.* **120**, 183003 (2018).
- [6] A. von Conta, A. Tehlar, A. Schletter, Y. Arasaki, K. Takatsuka, H.J. Wörner, *Nat. Commun.* **9**, 3162 (2018).
- [7] M.S. Schuurman, V. Blanchet, *Phys. Chem. Chem. Phys.* **24**, 20012 (2022).
- [8] H. Geiseler, H. Rottke, N. Zhavoronkov, W. Sandner, *Phys. Rev. Lett.* **108**, 123601 (2012).
- [9] A.H. Roos, Z. Hoque, E. Klimešová et al. *New J. Phys.* **25**, 013038 (2023).
- [10] V. Svoboda, N. Bhargava Ram, D. Baykushcheva, D. Zindel, M.D.J. Waters, B. Spenger, M. Ochsner, H. Herburger, J. Stohner, H.J. Wörner *Sci. Adv.* **8**, eabq2811 (2022).
- [11] M. Mudrich, F. Stienkemeier, *Int. Rev. Phys. Chem.* **33**, 301 (2014).
- [12] M.P. Ziemkiewicz, D.M. Neumark, O. Gessner, *Int. Rev. Phys. Chem.* **34**, 239 (2015).
- [13] B. Schütte, M. Arbeiter, A. Mermillod-Blondin, M.J.J. Vrakking, A. Rouzée, T. Fennel, *Phys. Rev. Lett.* **116**, 033001 (2016).
- [14] L. Jurkovičová, L.B. Ltaief, A.H. Roos et al., *Commun. Phys.* **7**, 26 (2024).
- [15] C. Medina, A.Ø. Lægdsmand, L.B. Ltaief et al., *New J. Phys.* **25**, 053030 (2023).
- [16] R. Antipenkov, E. Erdman, J. Novák et al., in: *Optica Advanced Photonics Congress 2022*, Optica Publishing Group, 2022, p. AW2A.4.
- [17] E. Klimešová, O. Kulyk, Z. Hoque et al., *Eur. Phys. J. Spec. Top.* **230**, 4183 (2021).
- [18] E. Klimešová, O. Kulyk, Y. Gu, L. Dittrich, G. Korn, J. Hajdu, M. Krikunva, J. Andreasson, *Sci. Rep.* **9**, 8851 (2019).
- [19] E. Klimešová, O. Kulyk, L. Dittrich, J. Andreasson, M. Krikunova, *Phys. Rev. A* **104**, L061101 (2021).
- [20] J. Nejd, U. Chaulagain, O. Hort et al., *Proc. SPIE* **11886**, 1188608 (2021).
- [21] J.H.D. Eland, O. Vieuxmaire, T. Kinugawa, P. Lablanquie, R.I. Hall, F. Penent, *Phys. Rev. Lett.* **90**, 053003 (2003).
- [22] J.H.D. Eland, R. Feifel, *Chem. Phys.* **327**, 85 (2006).
- [23] A.T.J.B. Eppink, D.H. Parker, *Rev. Sci. Instrum.* **68**, 3477 (1997).
- [24] A. Zhao, M. van Beuzekom, B. Bouwens et al., *Rev. Sci. Instrum.* **88**, 113104 (2017).
- [25] H. Bromberger, Ch. Passow, D. Pennicard et al., *J. Phys. B At. Mol. Opt. Phys.* **55**, 144001 (2022).
- [26] J. Lee, H. Köckert, D. Heathcote, D. Papat, R. Chapman, G. Karras, P. Majchrzak, E. Springate, C. Vallance, *Commun. Chem.* **3**, 72 (2020).
- [27] C. Schouder, A.S. Chatterley, M. Johnny, F. Hübschmann, A.F. Al-Refai, F. Calvo, J. Küpper, H. Stapelfeldt, *J. Phys. B At. Mol. Opt. Phys.* **54**, 184001 (2021).
- [28] ELI Beamlines Facility website.
- [29] Extreme Light Infrastructure ERIC website.